Band Bending in Conjugated Polymer Layers

Ilja Lange,[1] James C. Blakesley,[1,*] Johannes Frisch,[2] Antje Vollmer,[3] Norbert Koch,[2,3] and Dieter Neher[1,†]

[1]*Institut für Physik und Astronomie, Universität Potsdam, Karl-Liebknecht-Straße 24-25, 14476 Potsdam, Germany*
[2]*Institut für Physik, Humboldt-Universität zu Berlin, Brook-Taylor-Straße 6, 12489 Berlin, Germany*
[3]*BESSY II, Helmholtz-Zentrum für Materialien und Energie GmbH, Albert-Einstein-Straße 15, 12489 Berlin, Germany*

(Received 24 January 2011; published 25 May 2011)

We use the Kelvin probe method to study the energy-level alignment of four conjugated polymers deposited on various electrodes. Band bending is observed in all polymers when the substrate work function exceeds critical values. Through modeling, we show that the band bending is explained by charge transfer from the electrodes into a small density of states that extends several hundred meV into the band gap. The energetic spread of these states is correlated with charge-carrier mobilities, suggesting that the same states also govern charge transport in the bulk of these polymers.

DOI: 10.1103/PhysRevLett.106.216402 PACS numbers: 71.20.Rv, 71.55.Jv, 73.30.+y, 88.40.jr

The energy-level alignment at interfaces between organic semiconductors (OSCs) and electrodes determines many processes relevant to device performance. Contacts formed by spin-coating conjugated polymers onto weakly reactive electrodes commonly exhibit vacuum-level alignment (Schottky-Mott limit) when the work function of the electrode is well within the transport gap [commonly defined as the difference between the onsets of filled and empty states seen in photoemission spectroscopy (PES) and inverse photoemission spectroscopy] [1,2]. This implies that the density of interfacial gap states is low at such electrode-polymer contacts. It is believed that processing from solution causes a thin layer of surface contamination, which effectively prevents mixing of the polymer states with the continuum of metal states in the electrode. For such interfaces with weak electronic interaction, the energetics will be entirely determined by electron transfer between the electrode and occupied or unoccupied states in the OSCs.

Work by numerous groups indeed showed that the work function of a polymer-coated electrode, Φ_{OSC}, equals the work function of the contaminated substrate, Φ_{sub}, within a certain range $\Phi_{\mathrm{min}} < \Phi_{\mathrm{sub}} < \Phi_{\mathrm{max}}$, while it becomes constant and independent of the substrate work function when Φ_{sub} approaches the electron affinity or the ionization energy of the OSC [1–3]. As Φ_{min} and Φ_{max} consistently lie well within the transport gap, it was proposed that the Fermi level (E_F) becomes pinned at the level of energetically relaxed polaron states [4]. While this implies unexpectedly high relaxation energies, approaching 1 eV in some cases, Crispin *et al.* pointed out that polarons formed close to a metallic electrode will be stabilized by the mirror charge effects [5]. They also proposed that interfacial charge transfer creates polarons primarily in the first monolayer of polymer chains, while little or no charge transfer occurs to states in the bulk of the organic layer.

Recent PES investigations by Hwang *et al.* [6], however, revealed considerable band bending in polyfluorene copolymer films on high work function anodes. This phenomenon was ascribed to the accumulation of space charge in the OSC bulk by filling or emptying states in the tail of a continuous density of states (DOS) distribution. Studies of the DOS of OSCs often reveal Gaussian- or exponential-shaped tails which extend several hundreds of meV into the transport gap [7,8]. In the following, we refer to the part of the DOS that lies within the nominal transport gap as the density of tail states (DOTS). Those tail states are ascribed to energetic disorder caused by structural, conformational, or chemical defects in the organic film. Ueno and coworkers recently proposed that disorder-induced gap states control the E_F alignment at the contact [7].

According to recent numerical simulations, band bending caused by tail states can extend several tens of nanometers into the organic layer, accompanied by significant energetic displacement of the transport states in the OSC relative to the substrate E_F [9,10]. Surprisingly, few experimental studies have conclusively demonstrated band bending in OSCs [6,10–12]. PES yields precise information on the energetics at the electrode-OSC contact, but its application to study band bending in OSCs with thickness exceeding a few tens of nanometers tend to be problematic as sample charging may preclude accurate measurements. Here we apply the Kelvin probe method (KP) to study layers of four conjugated polymers (F8BT, PFTBTT, CN-ether-PPV, and Polyera$^{\mathrm{TM}}$ ActiveInk N2200) of a large range of thicknesses deposited on conducting substrates. Substrate work functions were varied from 3 to nearly 7 eV by using a range of metal (Ag, Au, Cr, Al, and Sm), metal oxide (MoO_3), and conductive polymer (Clevios$^{\mathrm{TM}}$ P VP AI 4083 and Clevios$^{\mathrm{TM}}$ HIL1.3) electrodes. KP measurements, in an N_2 atmosphere, were found to be highly reproducible, varying by less than ± 20 meV upon repetition of the experiments. For reference, ultraviolet PES (UPS) measurements were also carried out. For full experimental details, chemical structures, suppliers, and UPS valence spectra, see [13].

Figures 1(a)–1(d) show the measured Φ_{OSC} as a function of polymer film thickness d, with the uncoated electrode work function displayed at $d = 0$. For all polymers, band bending is seen when Φ_{sub} is very high or low, while little or no band bending is observed for electrodes with moderate Φ_{sub}. There is a small exception in the case of N2200, where weak band bending of 0.1–0.2 eV is seen even when E_F is well within the transport gap, indicating possible weak n-type doping. For all four polymers, the direction of band bending is reversed when switching from a low to a high work function electrode. We see that the work function increases (decreases) with layer thickness for low (high) Φ_{sub}, consistent with the formation of a negative (positive) space charge in the polymer film. The extent of the band bending for a given thickness of a given polymer is also independent of the exact chemical nature of the electrode. Our data show consistently that significant band bending occurs in layers of conjugated polymers, extending several tens of nanometers into the bulk, and that it must be related to the transfer of charges between the electrodes and the electronic states in the bulk of the polymer layer. Figures 1(e)–1(h) show Φ_{OSC} obtained for 75-nm-thick polymer films as a function of Φ_{sub}. All four curves have a ''Z-like'' shape, with $\Phi_{OSC} \approx \Phi_{sub}$ between (polymer-specific) upper and lower critical values of Φ_{sub} and Φ_{OSC} approximately constant outside this range. Clearly, band bending determines the lower and upper limits of the Z curve for thick films.

We were able to fit the data by using a simple model of charge transfer into the DOTS. Since the Kelvin potential defines the condition with no net current flow, E_F is constant throughout the polymer film and is aligned with the substrate E_F. The charge-carrier density n at a distance x from the electrode-OSC interface is then given by the convolution of the Fermi-Dirac distribution with the DOS of the polymer:

$$n(x) = \int_{-\infty}^{\infty} \frac{1}{1 + \exp[(E - E_F)/k_B T]} g[E + eV(x)]dE, \quad (1)$$

where E is energy, k_B is Boltzmann's constant, T is temperature, $g(E)$ is the model DOS, and $V(x)$ is the electrostatic potential. The latter is given by solving the one-dimensional Poisson's equation:

$$\frac{d^2V}{dx^2} = \frac{en(x)}{\varepsilon} \quad (2)$$

under the boundary condition that the electric field vanishes at the polymer surface. e is the elementary charge, and ε is the permittivity of the polymer film. We assume a relative permittivity of 3.5 for all polymers. Equations (1) and (2) are solved simultaneously to give the equilibrium

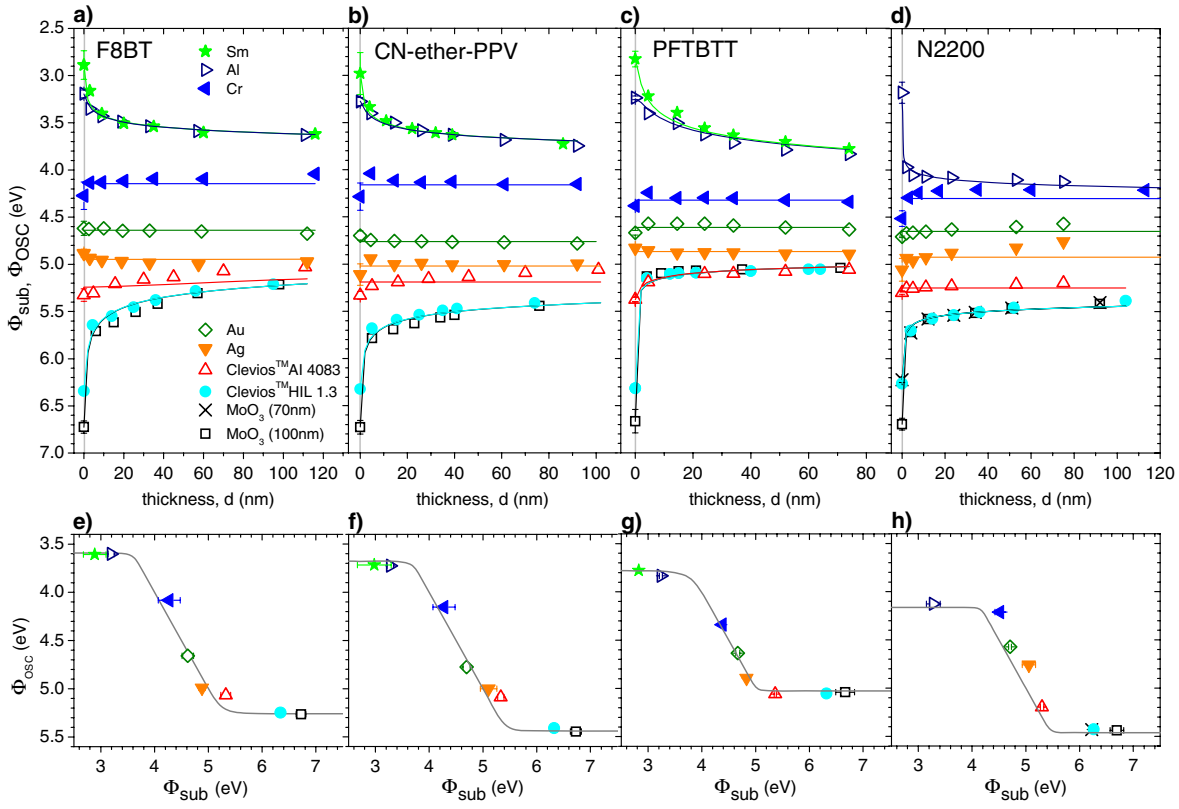

FIG. 1 (color online). Work function Φ_{OSC} of conjugated polymers on various substrates with work function Φ_{sub}. Symbols: KP measurements; solid lines: simulated results with Gaussian model DOS. (a)–(d) vs polymer thickness; (e)–(h) Φ_{OSC} on 75 nm polymer film (measurements interpolated) vs Φ_{sub}. Valence band onsets measured by UPS are 5.90, 6.10, 5.50, and 5.85 eV, respectively (see [13]).

distribution for charges that thermally diffuse into the polymer and the resulting electrostatic potential in the polymer film. $V(x = 0)$ is the potential drop across the interface accounting for interface dipoles (effectively changing Φ_{sub}). In the absence of interface dipoles, $V(0) = 0$. The difference between Φ_{OSC} and Φ_{sub} is given by $eV(d)$, which includes contributions from interface dipoles and space charge.

We have fitted our data by using either a Gaussian or an exponential model DOS. The former is

$$g(E) = \frac{N_0}{\sigma\sqrt{2\pi}} \exp\left[-\frac{(E - E_0)^2}{2\sigma^2}\right], \quad (3)$$

where N_0 is the integrated state density, σ is the width of the Gaussian, and E_0 is the center of the distribution. No analytical solution is possible in this case, and the set of equations was solved numerically to yield Φ_{OSC} as a function of Φ_{sub} and d. Setting N_0 to 10^{21} cm^{-3}, we varied E_0 and σ for both the highest occupied molecular orbital (HOMO)- and the lowest unoccupied molecular orbital (LUMO)-related DOTS to fit the data for all four polymers [solid lines in Figs. 1(a)–1(h)].

The exponential model distribution can be written as $g(E) \propto \exp(E/E_t)$, where E_t describes the width of the DOTS. For $E_t > k_B T$, Eq. (1) can be approximated by

$$n(x) = N_t \exp\left[\frac{eV(x) + E_F}{E_t}\right], \quad (4)$$

where N_t is a parameter related to the density and position of tail states. Adapting the approach by Ottinger, Melzer, and von Seggern [14], Eqs. (2) and (4) can be solved to express the work function as an inverse function of film thickness:

$$d = \sqrt{\frac{2E_t\varepsilon}{e^2 N_t}} \exp\left(\frac{\Phi_{OSC}}{2E_t}\right) \times \arccos\left\{\exp\left[\frac{\Phi_{sub} - eV(0) - \Phi_{OSC}}{2E_t}\right]\right\}. \quad (5)$$

The above equations are written in a sign convention of negative charge carriers. Again, we found that good fits to the data could be obtained by varying only E_t and N_t (Fig. S3, Ref. [13]).

Table I shows the best-fit values of σ and E_t obtained for the Gaussian and exponential model DOS, respectively, together with the approximate range of values. Since each model DOS has two variables, the width of the DOS can be varied by typically ±30% while adjusting its position to get a good fit. Furthermore, fitting is not able to distinguish a preference for a Gaussian or exponential DOS.

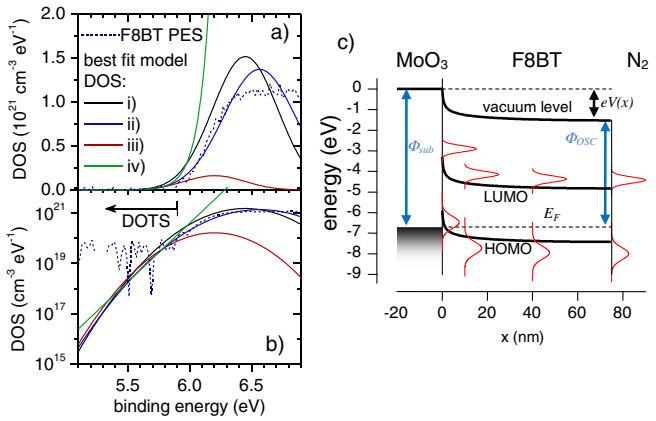

FIG. 2 (color online). (a),(b) Solid lines: Fitted model DOS of F8BT according to 4 different scenarios described in the text. Dashed lines: PES valence spectrum of F8BT (scaled to fit the model DOS at onset). (a) Linear scale; (b) logarithmic scale. There is a significant fitting uncertainty in the position of the density of states distribution but a small uncertainty in the DOTS below the limit of PES sensitivity. Also shown (c) is the energy diagram of 75 nm F8BT on MoO_3. Solid lines show the onsets of the HOMO- and LUMO-derived bands (black curves) (HOMO onset energy from UPS; LUMO onset from HOMO onset plus optical absorption maximum) and best-fit Gaussian model DOS at four depths (red curves). The potential V is calculated as described in the text.

Figure 2 illustrates the limits of this uncertainty. The KP measurements for F8BT on 100 nm MoO_3 were fitted by using a Gaussian model DOS under three different conditions: (i) a fit with no interface dipole, $N_0 = 10^{21}$ cm^{-3}; (ii) a fit with the same state density but with assuming a 1 eV interface dipole (corresponding to the change of the work function with ~5 nm coverage); and (iii) a fit with no interface dipole and $N_0 = 10^{20}$ cm^{-3} (a reasonable lower limit for the DOS). In each case, a good fit to the data could be achieved by varying the free parameters σ and E_0. The resulting fitted model DOS are displayed together with the best exponential model DOS (iv) and the valence photoemission spectrum of F8BT in Fig. 2. On a linear scale, the model DOS appear to differ greatly. However, when plotted on a logarithmic scale, all four models yield similar densities of tail states in the energy range of 5.2–5.7 eV.

TABLE I. Best-fit values of distribution parameters for Gaussian and exponential model DOS, respectively. The ranges of possible values that can fit to the data are given in brackets.

	F8BT		CN-ether-PPV		PFTBTT		N2200	
	HOMO	LUMO	HOMO	LUMO	HOMO	LUMO	HOMO	LUMO
σ (meV) (Gaussian)	340 (280–380)	140 (100–190)	200 (120–260)	160 (110–220)	<90	320 (250–420)	95 (65–125)	<65
E_t (meV) (exponential)	95 (80–110)	55 (40–75)	60 (40–90)	65 (45–90)	<40	115 (90–150)	50 (35–65)	<30

This is the energy range that determines band bending in the bulk of the polymer layer. We conclude that band bending is determined almost entirely by the energetic distribution of tail states, while it is relatively insensitive to the position and density of states at the center of the DOS.

Our calculations show that a broad DOTS (with a width well above k_BT) can be inferred sensitively from the analysis of the KP measurements. Alternatively, when the DOTS is very narrow (e.g., in a well-ordered material), the contribution to band bending from tail states is small compared to the space charge arising from thermal excitation of carriers into states in the organic layer above E_F. This case has been treated recently by Ottinger, Melzer, and von Seggern [14]. In this limit of ''thermally induced'' band bending, the curve of Φ_{OSC} vs d is very steep at small d and is almost flat for $d > \sim 10$ nm. This situation is seen for the LUMO of N2200 and the HOMO of PFTBTT. We cannot set a lower limit on the width of the DOTS in these two cases. Instead, we can be more precise about the positions of these bands and find that the onsets of N2200 LUMO- and PFTBTT HOMO-derived bands are at 3.8 ± 0.1 and 5.35 ± 0.2 eV, respectively. These compare well with measured values of 3.91 (from cyclic voltammetry [15]) and 5.5 ± 0.1 eV (from our own PES data). In all other cases, the observed band bending can be fitted only by a model DOS including tail states.

Studies of charge transport in disordered materials have shown that charge-carrier mobility is severely limited by the relaxation of carriers into tail states. This results in a pronounced density-, field-, and temperature-dependent mobility [16–18]. As a general example of this, we find distinct correlations between band bending measured here and charge transport reported on these polymers. For example, the analysis of band bending in PFTBTT reveals a wider DOTS for electrons and a narrower one for holes. This fits in with studies by Andersson *et al.*, who found a relatively high hole mobility in this polymer, while they were unable to measure any electron conduction at all [19,20]. F8BT and CN-ether-PPV both exhibit pronounced band bending, indicative of a broad DOTS for electrons and holes. Despite the large difference in the chemical structure, the parameters describing the width of the LUMO-related DOTS are rather comparable. This correlates well with previous charge transport measurements, which showed that electron transport was poor in both polymers and described by either trap sites with a characteristic energy of about 100 meV [21] or Gaussian energetic disorder, also with a distribution of about 100 meV [22]. The narrowest distribution of tail states of all was found for N2200, a material that has the highest electron mobility ever reported in a conjugated polymer [23,24].

In conclusion, we observed significant band bending in four different conjugated polymers when deposited on a substrate with a high or low work function. We propose that band bending depends on, and *only* on, the work function of the electrode and the electronic structure of the polymer film. Band bending as a function of layer thickness on different substrates was consistently explained by the transfer of charge from the electrode into tail states in the polymer bulk. The energetic spread of the tail states correlates well with charge-carrier mobilities reported in previous studies, suggesting that the states responsible for band bending also govern charge transport. Furthermore, our results support the hypothesis that space charge formed by occupation of tail states defines almost entirely the energetics near the electrode-polymer contact. DOTS derived from KP measurements could thus be more relevant to device properties than the onset of occupied and unoccupied states revealed from cyclic voltammetry or PES investigations.

The authors thank S. Janietz (Fraunhofer Institute IAP) for providing F8BT and PFTBTT, H.-H. Hörhold (Universität Jena) for CN-ether-PPV, Z. Chen and A. Facchetti (Northwestern University and Polyera) for N2200 (Polyera ActivInk N2200), and A. Elschner (Heraeus Clevios GmbH) for HIL1.3.

*james.blakesley@physics.org
†neher@uni-potsdam.de

[1] J. Hwang, A. Wan, and A. Kahn, Mater. Sci. Eng., R **64**, 1 (2009).
[2] S. Braun, W. R. Salaneck, and M Fahlman, Adv. Mater. **21**, 1450 (2009).
[3] S. Rentenberger *et al.*, J. Appl. Phys. **100**, 053701 (2006).
[4] C. Tengstedt *et al.*, Appl. Phys. Lett. **88**, 053502 (2006).
[5] A. Crispin *et al.*, Appl. Phys. Lett. **89**, 213503 (2006).
[6] J. Hwang *et al.*, J. Phys. Chem. C **111**, 1378 (2007).
[7] T. Sueyoshi *et al.*, Appl. Phys. Lett. **95**, 183303 (2009).
[8] I. N. Hulea *et al.*, Phys. Rev. Lett. **93**, 166601 (2004).
[9] J. C. Blakesley and N. C. Greenham, J. Appl. Phys. **106**, 034507 (2009).
[10] G. Paasch *et al.*, J. Appl. Phys. **93**, 6084 (2003).
[11] H. Ishii *et al.*, Phys. Status Solidi A **201**, 1075 (2004).
[12] R. Schlaf *et al.*, J. Appl. Phys. **86**, 1499 (1999).
[13] See supplemental material at http://link.aps.org/supplemental/10.1103/PhysRevLett.106.216402 for experimental methods, chemical structures, UPS valence spectra, and fits with exponential DOS.
[14] O. M. Ottinger, C. Melzer, and H. von Seggern, J. Appl. Phys. **106**, 023704 (2009).
[15] Z. Chen *et al.*, J. Am. Chem. Soc. **131**, 8 (2009).
[16] C. Tanase *et al.*, Phys. Rev. Lett. **91**, 216601 (2003).
[17] H. Bässler, Phys. Status Solidi B **175**, 15 (1993).
[18] P. Mark and W. Helfrich, J. Appl. Phys. **33**, 205 (1962).
[19] L. M. Andersson and O. Inganäs, Appl. Phys. Lett. **88**, 082103 (2006).
[20] L. M. Andersson, F. Zhang, and O. Inganäs, Appl. Phys. Lett. **91**, 071108 (2007).
[21] R. Steyrleuthner, S. Bange, and D. Neher, J. Appl. Phys. **105**, 064509 (2009).
[22] J. C. Blakesley, H. S. Clubb, and N. C. Greenham, Phys. Rev. B **81**, 045210 (2010).
[23] H. Yan *et al.*, Nature (London) **457**, 679 (2009).
[24] R. Steyrleuthner *et al.*, Adv. Mater. **22**, 2799 (2010).